Twisted cucurbit[14]uril: a new type of CTE macrocycle for Fe^{3+} sensing

Wei Zhang[a‡], Yang Luo [a‡], Mao-Xia Yang [a], Wen-Hao Lin [a], Carl Redshaw [b], Xin-Long Ni [a], Ying Huang[a], Zhu Tao [a] and Xin Xiao [a]*

[a] *Key Laboratory of Macrocyclic and Supramolecular Chemistry of Guizhou Province, Guizhou University, Guiyang 550025, China*.

[b] *Department of Chemistry, University of Hull, Hull HU6 7RX, U.K*

[‡] *Joint first authors*

ABSTRACT

Clustering-triggered emission (CTE) luminophores have aroused great attention given they are unconventional luminescence compounds without significant conjugation. In this work, the luminescence phenomenon of twisted cucurbit[14]uril (*t*Q[14]) is reported for the first time, and reveals it to be a new CTE compound. We systematically studied the luminescence characteristics and mechanism of *t*Q[14] in formic acid, and confirmed that the clustering emission of *t*Q[14] arises via multiply n-π* interactions and hydrogen bonding. We then demonstrated the potential application of this system as an Fe^{3+} sensor, and the detection of limit (LOD) was found to be 1.71×10^{-5} M. This work not only reveals new characteristics and the mechanism of the clustering emission of *t*Q[14], but also provides new insights into how to utilize the clustering emission of *t*Q[14] for the construction of new types of macrocyclic luminescence systems.

INTRODUCTION

Traditional luminescent materials are fluorophores possessing significant conjugated structures, typically (heterocyclic) aromatic hydrocarbons, [1-2] while some non-traditional emitters and polymers with non-conjugated structures can also emits strong luminescence following aggregation. Recently, Wang's group proposed the new concept of clustering-triggered emission (CTE) [3] to explain this aggregation-induced emission behavior for non-traditional luminescence [4]. Namely, the clustering of non-aromatic chromophores induces effective interactions among electron-rich moieties (*i. e.* N, O, P, S) including hydrogen bonding, n-π* interactions, dipole-dipole interactions *etc.* [5-7], which enhances the overlapping of electron clouds as well as extending the conjugation and results in the formation of rigidified conformations and bright glowing materials. CTE compounds discovered to-date mainly include dendritic macromolecules, starch, cellulose, sodium alginate, chitosan, amino acids, etc. [8]. These materials have been applied in sensors, bioimaging technology as well as in smart materials, and there are clearly prospects for the development of more useful luminescent materials [9-11].

Twisted cucurbit[14]uril (*t*Q[14]) [12], as a new member of the cucurbit[*n*]uril (Q[*n*]) family [13-18], is a new potential CTE molecule. *t*Q[14] is synthesized by the condensation of glycourils and formaldehyde in acidic medium, and contains 14 glycoluril units and 28 methylene bridges [19]. Such a high degree of polymerization of *t*Q[14] spawned its unique structure *viz* a distorted shape, double cavities, multiple carbonyl portals rich in C=O and a large outer surface area rich in $CH_{methine}$ and $CH_{2methylene}$ groups. This provides more active sites for n-π* interactions (C=O···C=O) and hydrogen bonding (C=O···$CH_{methine}$, C=O··· $CH_{2methylene}$). Our group collectively referred to these interactions as self-induced outer surface interactions of Q[*n*] (OSIQ) [20-21]. Therefore, the driving force for the fluorescence

of *t*Q[14] is self-induced OSIQ (n-π* interactions and hydrogen bonding). These unconventional chromophores carrying π electrons at the carbonyl portals of *t*Q[14] can be aggregated through n-π* interactions, and subsequently the overlap with $CH_{methine}$ and $CH_{2methylene}$ groups carrying (n) lone pair electrons at the outer surface of *t*Q[14] through hydrogen bonding. This results in a rigidified conformation and a bright glow.

In this work, the unusual luminescence behavior of *t*Q[14] in water, DMSO and formic acid is reported for the first time. Both the fluorescence and the dynamic light scattering (DLS) reveals that self-induced OSIQ (n-π* interaction and hydrogen bonding) trigger the CTE effect, which results in a luminescent *t*Q[14]. The *t*Q[14] can be further used as a simple fluorescence probe for the detection of Fe^{3+} [22]and the detection of limit (LOD) is calculated as 1.71×10^{-5} M. This unprecedented major discovery for *t*Q[14] open up a new pathway for Q[*n*] applications that can now be directly applied for sensing, porous materials, hydrogel and other yet unknown fields.

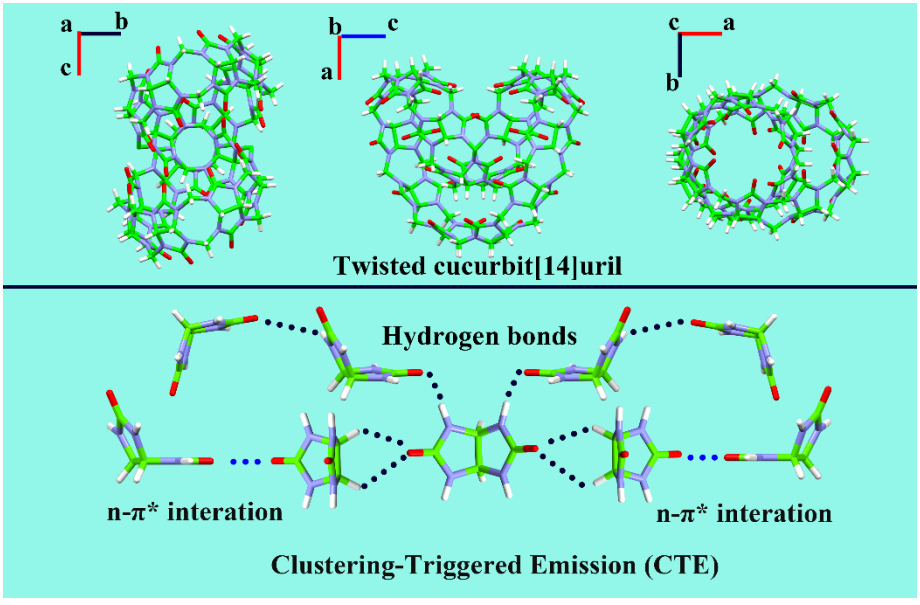

Scheme 1 The structure of *t*Q[14] and the illustration of interactions within clustering *t*Q[14].

RESULTS AND DISCUSSION

In order to better visualize the luminescence behavior of *t*Q[14] in different solutions, we first selected three common solutions (c = 0.5 mM H_2O, DMSO, HCOOH) that can dissolve *t*Q[14]. As shown in Figures 2a, b, *t*Q[14] emits weak blue fluorescence, and the corresponding fluorescence intensity in DMSO and water is as low as 116.4 a.u. and 72.3 a.u., respectively. However, *t*Q[14] in formic acid exhibits stronger blue fluorescence, and its fluorescence intensity is 407.6 a.u. The stronger blue fluorescence of *t*Q[14] in formic acid is likely due to the fact that *t*Q[14] has more intermolecular forces (multiple hydrogen bonding, n-π* interactions and dipole-dipole interactions *etc*.) than are present in H_2O and DMSO [6]. Meanwhile, the formed clusters of *t*Q[14] in formic acid were further studied by fluorescence spectroscopy. As shown in Figure 1c, the fluorescence intensity and the max emission wavelength of *t*Q[14] in formic acid with different excitation wavelengths remains unchanged, consistent with the presence of the same aggregation structure in formic acid.

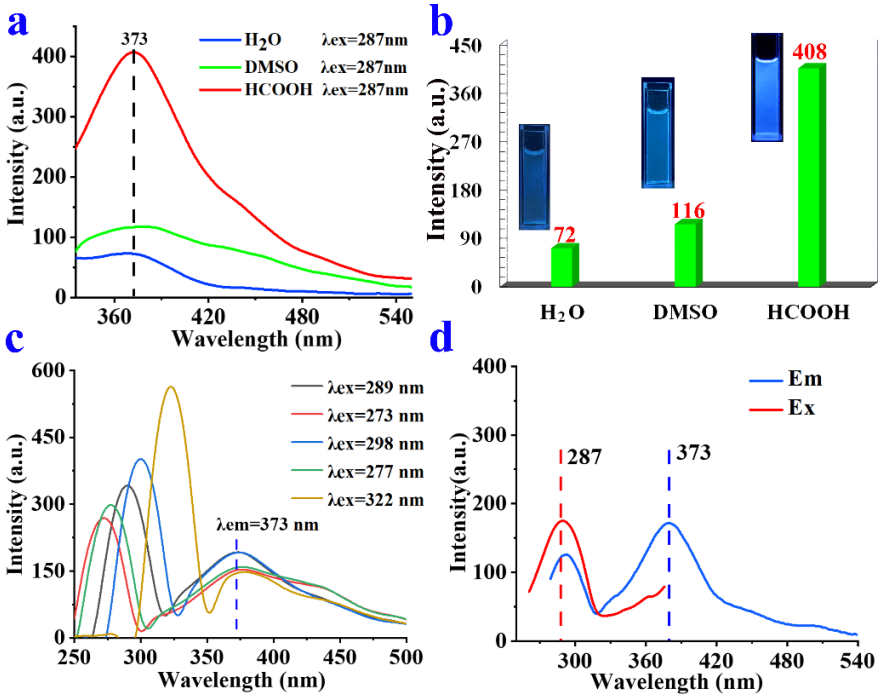

Figure 1. Fluorescence spectra: (a, b) different solvents and histograms of *t*Q[14]; (c) different excitation wavelengths of *t*Q[14] (0.5 mM, HCOOH/methanol F_{HCOOH} = 99 %); (d) Excitation (E_x) and emission (E_m) spectra of *t*Q[14] (0.5 mM, HCOOH/methanol F_{HCOOH} = 99 %).

To better visualize and verify the CTE behavior of *t*Q[14] in the aggregated excited states, the fluorescence of *t*Q[14] was first examined in a mixed solution of HCOOH/methanol with different formic HCOOH components (Figure 2a). The emission of *t*Q[14] (0.5mM) was very weak in methanol, and it increased slowly when the HCOOH content was less than 70 vol %. However, when the water content increased from 70 to 99 vol %, the fluorescence intensity of *t*Q[14] enhanced significantly caused by the intriguing CTE effect owing to the formation of clustering at this concentration [23]. Simultaneously, an obvious Tyndall effect could be observed (Figure 2b, inset). The formic acid solution of *t*Q[14] (0.5 mM) showed strong blue fluorescence under λ_{ex} =287nm. These observations are fully consistent with the well-established CTE mechanism, and such behavior can also be directly visualized under a 365 nm UV lamp (Figure 2a, inset). Dynamic light scattering (DLS) profiles revealed the formation of clustering with average sizes increasing from a hydrodynamic diameter (D*h*) of 53 nm for F_{HCOOH} = 0 % to 560 nm for F_{HCOOH} = 99 % (Figure 2c). The clustering emission phenomena of *t*Q[14] in the solid-state was also studied. Under sunlight, *t*Q[14] appears as a white powdery solid, whereas it emits a bright blue fluorescence under excitation with UV light at 365 nm (Figure 2d).

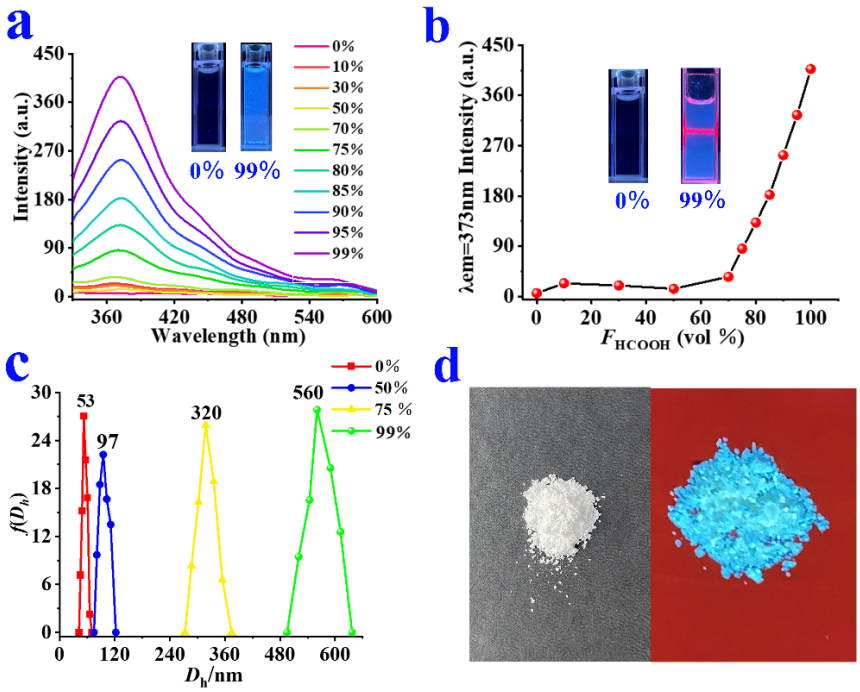

Figure 2 CTE behavior of *t*Q[14]: (a) emission spectra of solutions in HCOOH/methanol with increasing F_{HCOOH} (0.5 mM, λ_{ex} = 287 nm); (b) curve showing the emission intensity changes and photographs taken under 365 nm UV irradiation (inset); (c) selected DLS profiles of solutions as a function of the volume F_{HCOOH} = 99 %; (d) Photographs of the *t*Q[14] solid obtained under daylight and UV light at 365 nm.

To further understand the CTE process and mechanism, the crystal structures of clustering *t*Q[14] we obtained previously are revisited [24]. The crystal structure of the supramolecular framework constructed by the *t*Q[14] molecules is made up of 2D frameworks (Figure 3b), in which each *t*Q[14] molecule in the framework can interact with four adjacent *t*Q[14] molecules via self-induced OSIQ. As shown in Figure 3b, each carbonyl oxygen atom (C=O) in *t*Q[14] is anchored to C=O; and is involved in C=O···$CH_{methine}$; C=O···$CH_{2methylene}$ with another macrocyclic unit. Such clustering may afford electronic interactions such as C=O···C=O; C=O···$CH_{methine}$; there are C=O···$CH_{2methylene}$ short contacts among the n-π* interaction electrons, which enhance the through space electronic conjugation and simultaneously rigidify the conformations. Meanwhile, effective intra- and intermolecular hydrogen bonds of *t*Q[14] are present, which both rigidify the molecular conformations and facilitate through space

conjugation among adjoining n-π* interactions. Consequently, these non-aromatic luminophores bearing extended conjugations and rigidified conformations can be excited when forming clusters and produce visible emission when irradiated.

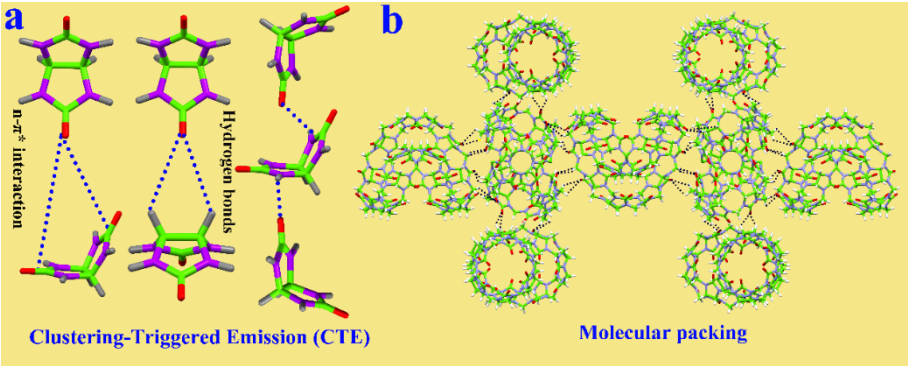

Figure 3 (a) Molecular packing with multiple intermolecular C=O···C=O, C=O···$CH_{methine}$ interactions and C=O···$CH_{2methylene}$ interactions in the crystal structure of *t*Q[14]; (b) crystal structures of the supramolecular framework constructed by *t*Q[14].

Using macrocyclic *t*Q[14] as new fluorescent probe, transition metal ions were chosen to evaluate their universal sensing capability for guest species in formic acid solution. Use common metal ions (c = 0.1 mM), as shown in Figure 4a, only the addition of Fe^{3+} led to the fluorescence of *t*Q[14] decreasing. In particular, the major emission band rapidly decreased and led to a quenching efficiency 95.47 % at 6.0 equiv. (Figure S4), indicating strong selectivity of *t*Q[14] towards Fe^{3+}. Meanwhile, the fluorescence titration of *t*Q[14] *vs* Fe^{3+} was monitored (Figure 4b). On increasing the concentration of Fe^{3+}, the fluorescence of *t*Q[14] at λ_{em} = 373 nm decreased from 305.8 a.u. to 17.4 a.u. (ΔI = 288.4 a.u.), whilst the corresponding titration curve exhibited a good linear trend. This detection method not only shows a lower detection of limit (LOD) is 1.71×10^{-5} M (σ = 4.4974) (Figure S7) with a good linear fitting (y=7.89x+0.17, R^2 = 0.99), but also exhibits good anti-interference towards other ions (Figure S5).

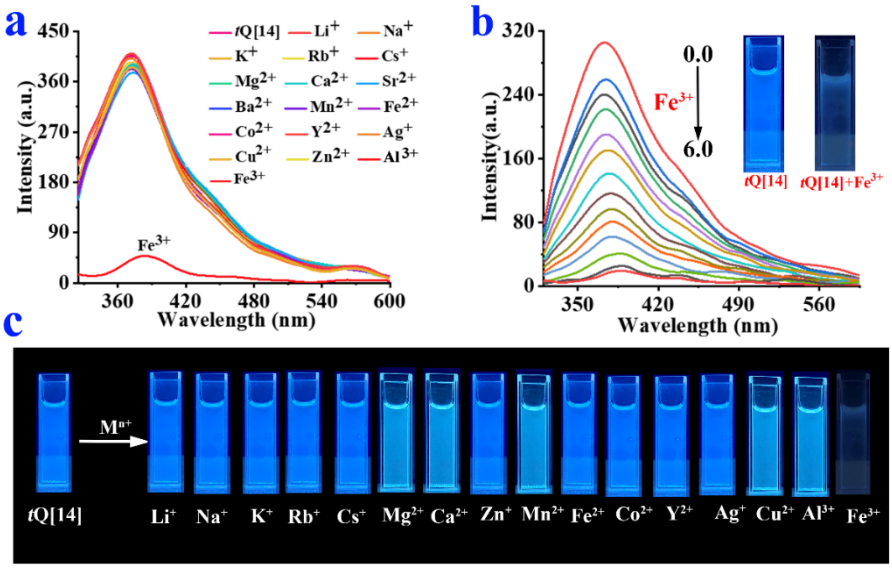

Figure 4 (a) Fluorescence spectra of *t*Q[14] (0.5 mM) towards 6 equivalents of different M^{n+} (3.0 mM); (b) Fe^{3+} sensing by *t*Q[14] of fluorescence titration; (c) Photographs of the above formic acid solutions illuminated by the UV lamp at 365 nm.

To further explore the fluorescence quenching mechanism, we performed several investigations. Although single crystals were not obtained from the mixture solution of *t*Q[14] and Fe^{3+} ions, we acquired spectroscopic signals and DLS data (Figure S9). The average hydrodynamic diameter of the aggregates was dramatically reduced to 227 nm after quenching of the sample *t*Q[14] (F_{HCOOH} = 99 %, D*h* = 560 nm), which is comparable to the molecular aggregation between F_{HCOOH} = 50 % and 70 % with a D*h* value of 97 nm and 320 nm, respectively. This finding may suggest that the disassembly of a highly aggregated state resulted in emission quenching of *t*Q[14] upon addition of Fe^{3+} ions. Subsequently, the absorption of Fe^{3+} and the emission spectrum of *t*Q[14] were measured (Figure S10). A significant overlap could be noted, which indicates that the efficient absorption of Fe^{3+} hinders the excitation of *t*Q[14] at 373 nm resulting in the quenching of its fluorescence [25-26]. Due to the existence of size-selective cavities and O-donating sites in macrocyclic *t*Q[14], we envisaged that they would be able to exhibit a luminescence response to the stimuli of organic guest species in polar media.

CONCLUSION

In conclusion, *t*Q[14] at high concentrations is affected by self-induced OSIQ and further aggregates into a fluorescence complex at 373 nm with a unique CTE effect. On increasing the concentration of *t*Q[14], the fluorescence as well as particle size increase significantly, indicating that an efficient cluster-induced emission effect is present within the clustering *t*Q[14] complex. Subsequently, the mechanism of the CTE process was inferred by the crystal structure of clustering *t*Q[14]. The C=O (π electrons) on the carbonyl portals of *t*Q[14] could be aggregated with each other through n-π* interactions, and C=O subsequently overlaps with the $CH_{methine}$ and $CH_{2methylene}$ groups (n electrons) on the outer surface of *t*Q[14] through hydrogen bonding, resulting in the fluorescence of *t*Q[14]. Meanwhile, *t*Q[14] can be used as a probe for detecting Fe^{3+}, and the detection of limit is as low as 1.71×10^{-5} M. This work not only reveals new characteristics and mechanism of the clustering emission of *t*Q[14], but also provides new insights into how to utilize the clustering emission of *t*Q[14] for the construction of new types of macrocyclic luminescence systems.

Corresponding Author

* Corresponding author: gyhxxiaoxin@163.com

Author Contributions

The manuscript was written through contributions of all authors. All authors have given approval to the final version of the manuscript. ‡These authors contributed equally.

ACKNOWLEDGEMENTS

This work was supported by the National Natural Science Foundation of China (No. 21861011, 21871064, 22061009) and the Innovation Program for High-level Talents of Guizhou Province (No. 2016-5657). CR thanks the EPSRC for an Overseas Travel Grant (EP/R023816/1).

CONFLICTS OF INTEREST

There are no conflicts to declare.

REFERENCES

[1] J. Luo, Z. Xie, J. W. Lam, L. Cheng, H. Chen, C. Qiu, H. S. Kwok, X. Zhan, Y. Liu, D. Zhu, B. Z. Tang, Aggregation-induced emission of 1-methyl-1,2,3,4,5-pentaphenylsilole, *Chem. Commun*. 37 (2001), 1740-17401.

[2] H. Bai, W. He, J. H. C. Chau, Z. Zheng, R. T. K. Kwok, J. W. Y. Lam, B. Z. Tang, AIEgens for microbial detection and antimicrobial therapy, *Biomaterials.* 268 (2021), 120598.

[3] Q. Zhou, B.Y. Cao, C. X. Zhu, S. Xu, Y. Y Gong, W. Z. Yuan, Y. M. Zhang, Clustering-triggered emission of nonconjugated polyacrylonitrile, *Small.* 12 (2016), 6586-6592.

[4] Y. Y. Gong, Y. Q. Tan, J. Mei, Y. R. Zhang, W.Z. Yuan, Y. M. Zhang, B. Z. Tang, Room Temperature Phosphorescence from Natural Products: Crystallization Matters, *Sci. China: Chem.* 56 (2013), 1178-1182.

[5] X. H. Chen, W. J. Luo, H. L. Ma, Q. Peng, Z. Y. Wang, Y. M. Zhang, Prevalent Intrinsic Emission from Nonaromatic Amino Acids and Poly (amino acids), *Sci. China: Chem*. 61 (2018), 351-359.

[6] X. Y. Dou, Q. Zhou, X. H. Chen, Y. Q. Tang, X. He, P. Lu, K. Y. Sun, B.Z. Tang, Y. M. Zhang, W. Z. Yuan, Clustering-triggered emission and persistent room temperature phosphorescence of sodium Alginate, *Biomacromolecules*. 19 (2018), 2014-2022.

[7] Y. Z. Wang, B. Xin. X. H. Chen, S. Y. Zheng, Y. Yuan, Zhang, M.; W. Z. Emission and emissive mechanism of nonaromatic oxygen clusters, *Macromol. Rapid. Commun*. 39 (2018), 1800528.

[8] S. Y. Tao, S. J. Zhu, T. L. Feng, B. Yang, Crosslink-Enhanced Emission Effect on Luminescence in Polymers: Advances and Perspectives, *Angew. Chem., Int. Ed*. 59 (2020), 9826-9840.

[9] L. F. Xu, X. Liang, S. L. Zhong, Y. Gao, Clustering-Triggered Emission from Natural Products: Gelatin and Its Multifunctional Applications, *ACS Sustainable Chem. Eng*. 8 (2020), 18816-18823.

[10] X. H. Chen, T. J. Yang, J. l. Lei, X. D. Liu, Z. H. Zhao, Z. Y. Xue, W. H. Li, Y. M. Zhang, W. Z. Yuan, Clustering-Triggered Emission and Luminescence Regulation by Molecular Arrangement of Nonaromatic Polyamide-6, *J. Phys. Chem. B*. 124 (2020), 8928-8936.

[11] Z. H. Zhao, X. H. Chen, Q. Wang, Y. M. Zhang, W. Z. Yuan, Sulphur-containing nonaromatic polymers: clustering-triggered emission and luminescence regulation by oxidation, *Polym. Chem.*10 (2019), 3639.

[12] X. J. Cheng, L. L. Liang, K. Chen, N.N. Ji, X. Xiao, J.X. Zhang, Y. Q. Zhang, S. F. Xue, Q. J. Zhu, X. L. Ni, Z. Tao, Twisted cucurbit [14] uril, *Angew. Chem., Int. Ed.* 52 (2013), 7393.

[13] R. H. Gao, Y. Huang, K. Chen, Z. Tao, Cucurbit[n]uril/metal ion complex-based frameworks and their potential applications, *Coord. Chem. Rev*. 437 (2021), 213741.

[14] M. Liu; L. X. Chen; X. Xiao, Z. Tao, C. Redshaw, Polymeric self-assembled cucurbit[*n*]urils: Synthesis, structures and applications, *Coord. Chem. Rev.* 434 (2021), 213733.

[15] M. Liu, L. X. Chen, P. H. Shan, C. J. Lian, Z. H. Zhang, Z. Tao, X. Xiao, Pyridine Detection Using Supramolecular Organic Frameworks Incorporating Cucurbit[10]uril, *ACS Appl. Mater. Inter*. 13 (2021), 7434-7442.

[16] H. Zhu, Z. H. Mao, J. Chen, J. J. Hu, X. J. Hu, K. Koh, H. X. Chen. Cucurbit[7]urils induced bimetallic nanoparticles network for ultra-sensitive detection of Caspase-3 based on surface plasmon resonance, *Microchemical. J.* 171 (2021), 106792.

[17] X. D. Zhang, K. Chen, W. Y. Sun. Potential Applications of Cucurbit[n]urils and Their Derivatives in the Capture of Hazardous Chemicals, Chem. Eur. J. 27 (2021), 5107-5119.

[18] C. J. Lian, W. T. Xu, Y. Luo, X. Y. Zhu, Y. Fan, C. Redshaw, Z. Tao, X. Xiao. Detection of the pesticide dodine using a cucurbit[10]uril-based fluorescent probe, *Microchemical. J*. 167 (2021), 106309.

[19] H. Cong, X. L. Ni, X. Xiao, Y. Huang, Q. J. Zhu, S. F. Xue, Z. Tao, L.F. Lindoy, G. Wei, Synthesis and separation of cucurbit[*n*]urils and their derivatives, *Org. Biomol. Chem.* 14 (2016), 4335-4364.

[20] X. L. Ni, X. Xiao, H. Cong, Q. J. Zhu, S. F. Xue, Z. Tao, Self-Assemblies Based on the "Outer-surface interactions" of cucurbit[*n*]urils: new opportunities for supramolecular architectures and materials, *Acc. Chem. Res.* 47(2014), 1386-1395.

[21] Y. Huang, R. H. Gao, M. Liu, L. X. Chen, X. L. Ni, X. Xiao, H. Cong, Q. J. Zhu, K. Chen, Z. Tao, Cucurbit[n]uril-based supramolecular frameworks assembled through outer-surface interactions, *Angew. Chem. Int. Ed.* 133 (2021), 15294-15319.

[22] L. Lin, D. X. Chen, C. F. Lu, X. X. Wang. Fluorescence and colorimetric dual-signal determination of Fe^{3+} and glutathione with MoSe2@Fe nanozyme, *Microchemical. J.* 177 (2022), 107283.

[23] J. Mei, L. C. Leung, T. K. Ryan, W. Y. Jacky, B. Z. Tang, Aggregation-Induced Emission: Together We Shine, United We Soar, *Chem. Rev*. 115 (2021), 11718-11940.

[24] S. C. Qiu, K. Chen, Wang, Y. Z. Y. Hua, F. Li, Y. Huang, Z. Tao, Y. J. Zhang, W. Wei, Crystal structure analysis of twisted cucurbit[14]uril conformations, *Inorganic Chemistry Communications.* 86 (2017), 49-53.

[25] W. Zhang, Y. Luo, Y. Zhou, M. Liu, B. Bian, Z. Tao, X. Xiao, A highly selective fluorescent chemosensor probe for detection of Fe^{3+} and Ag^{+} based on supramolecular assembly of cucurbit [10] uril with a pyrene derivative, *Dyes and Pigments*. 176 (2020), 108235.

[26] J. F. Chen, G. Y. Meng, Q. Zhu, S. H. Zhang, P. K. Chen, Pillar[5]arenes: a new class of AIEgen macrocycles used for luminescence sensing of Fe^{3+} ions, *J. Mater. Chem. C*. 7 (2019), 11747-11751.